Diagnostic Pathology

RESEARCH

Open Access

Prognostic and immune infiltration implications of *SIGLEC9* in SKCM

Peipei Yang[1†], Yunhui Jiang[2†], Rong Chen[3†], Junhan Yang[1], Mengting Liu[1], Xieping Huang[1], Ganglin Xu[1*] and Rui Hao[4*]

Abstract

The occurrence and progression of skin cutaneous melanoma (SKCM) is strongly associated with immune cells infiltrating the tumor microenvironment (TME). This study examined the expression, prognosis, and immune relevance of *SIGLEC9* in SKCM using multiple online databases. Analysis of the GEPIA2 and Ualcan databases revealed that *SIGLEC9* is highly expressed in SKCM, and patients with high *SIGLEC9* expression had improved overall survival (OS). Furthermore, the mutation rate of *SIGLEC9* in SKCM patients was found to be 5.41%, the highest observed. The expression of *SIGLEC9* was positively correlated with macrophages, neutrophils and B cells, CD8 + T cells, CD4 + T cells, and dendritic cells, according to TIMER. Based on TCGA-SKCM data, we verified that high *SIGLEC9* expression is closely associated with a good prognosis for SKCM patients, including overall survival, progression-free interval, and disease-specific survival. This positive prognosis could be due to the infiltration of immune cells into the TME. Additionally, our analysis of single-cell transcriptome data revealed that *SIGLEC9* not only played a role in the normal skin immune microenvironment, but is also highly expressed in immune cell subpopulations of SKCM patients, regulating the immune response to tumors. Our findings suggest that the close association between *SIGLEC9* and SKCM prognosis is primarily mediated by its effect on the tumor immune microenvironment.

Keywords Skin cutaneous melanoma, Tumor microenvironment, SIGLEC9, Single cell, Tumor infiltrating immune cells

Introduction

Skin cutaneous melanoma (SKCM) is a malignancy that commonly presents as a tumor, characterized by the active proliferation of tumor cells, evasion of immune surveillance, and an increased likelihood of both recurrence and metastasis [1, 2]. Cancer development is heavily influenced by the intricate interplay between tumors, stroma, and the immune system. SKCM is distinguished by its high mutation burden, neoantigen load, and diverse immune infiltration patterns [3, 4]. The use of immunotherapy checkpoint inhibitors targeting PD-1, CTLA-4, and PD-L1 has become more prevalent in SKCM treatment, resulting in significant enhancements in both survival rates and quality of life [5, 6].

SKCM is strongly linked to immune response genes and tumor-associated genes, which play a critical role in its onset and progression [7]. The Tumor microenvironment

†Peipei Yang, Yunhui Jiang and, Rong Chen contributed equally to this work.

*Correspondence:
Ganglin Xu
jmganglinxu@163.com
Rui Hao
825993347@qq.com
[1] Department of Dermatology, Jingmen People'S Hospital &, Jingchu University of Technology Affiliated Central Hospital, Jingmen 448000, China
[2] Department of Pathology, Jingmen People'S Hospital &, Jingchu University of Technology Affiliated Central Hospital, Jingmen 448000, China
[3] Department of Clinical Laboratory, Jingmen People'S Hospital &, Jingchu University of Technology Affiliated Central Hospital, Jingmen 448000, China
[4] Department of Oncology, Xiangyang Central Hospital, Affiliated Hospital of Hubei University of Arts and Science, Xiangyang 441021, China

(TME) consists of a diverse interplay between cell types, such as fibroblasts, endothelial cells, and immune cells, as well as extracellular components like cytokines, growth factors, and hormones, which collectively regulate the occurrence, development, and metastasis of many tumors, including SKCM [8]. Among the diverse cellular components of the TME, immune cells are the most abundant non-tumor cells, including innate immune cells like tumor-associated macrophages and neutrophils, antigen-presenting cells examples of innate immune cells include dendritic cells, while T cells and B cells are examples of acquired immune cells [9, 10]. The dynamic interaction between infiltrating immune cells in the TME and tumor cells, as well as other cell types, significantly impacts tumor progression [11, 12]. Thus, targeting immune cells within the TME holds promising potential as a strategy for cancer treatment.

Changes in the surface glycosylation patterns of malignant tumor cells, which are present on both immune regulatory cells and tumor cells, can potentially impact tumor immunity by directly interfering with the interaction between lectins (glycan-binding proteins) on their surfaces [13, 14]. One noteworthy point is that while normal T cells have low expression of the *SIGLEC* family, T cells that infiltrate tumor cells in the TME show high expression of *SIGLEC9*. Additionally, inhibitory receptors such as PD-1 are also expressed in this pattern. Targeting *SIGLEC9* has the potential to enhance the anti-tumor immune response. Furthermore, a study reveals a significant positive association between *SIGLEC9* expression and *CD8*+T cells, as well as *CD4*+memory activated T cells within the TME [15]. *SIGLEC9* is currently recognized to have a close association with the tumor immune microenvironment and has the potential to impact the prognosis of various tumors. Targeting *SIGLEC9* has been demonstrated to modulate the function of immune cells that infiltrate the TME, thereby influencing tumor invasion, metastasis, and immune metabolism [16–19]. Moreover, studies on SKCM have revealed that *SIGLEC9* can also regulate the anti-tumor effects of effector memory *CD8*+T cells [20, 21]. However, there is insufficient research on the mechanisms underlying the role of *SIGLEC9* in the development of SKCM and its interaction with immune cells that infiltrate the TME. Additionally, the comprehensive interactions and underlying molecular mechanisms involving immune cells and immune checkpoints in relation to *SIGLEC9* remain unclear.

This study integrates data from various online public databases and examines the prognostic significance and immune infiltration role of *SIGLEC9* in SKCM patients by utilizing SKCM bulk RNA and The Cancer Genome Atlas (TCGA) database's clinical data. Our objective was to examine the expression of *SIGLEC9* at the single-cell level in cells of normal skin and SKCM to provide a reference for targeted therapy of SKCM.

Materials and methods

GEPIA2 database

GEPIA2 (http://gepia2.cancer-pku.cn/#index, accessed on 16 Jan 2024) is an improved version of GEPIA, which integrates 461 SKCM patient tissue samples and 1 normal skin sample from TCGA database, along with 557 normal skin samples sourced from the Genotype-Tissue Expression Project (GTEx) database, to provide a more comprehensive analysis of gene expression across different cancer types. Follow the standard operating procedures [22] to analyze the discrepancies in *SIGLEC9* expression levels between SKCM and normal skin tissue, and evaluate the impact of *SIGLEC9* expression on both overall survival (OS) and disease free survival (DFS).

Ualcan database

By integrating TCGA transcriptomics and patient clinical information, the Ualcan database (http://ualcan.path.uab.edu/index.html, accessed on 16 Jan 2024) provides researchers with the ability to analyze gene expression levels, compare the expression differences between cancerous and normal tissue samples, and evaluate their association with clinical outcomes [23]. We consulted the Ualcan database manual to confirm the correlation between *SIGLEC9* expression and the OS of SKCM patients.

Data retrieval and analysis

We retrieved SKCM transcriptome and clinical data from TCGA database and excluded the data that had zero follow-up time or incomplete clinical information (accessed on 30 December 2023). We employed the R package 'survival' (version 4.1.3) to stratify patients into high and low *SIGLEC9* expression groups by dividing them based on the median value of *SIGLEC9* expression. Subsequently, we compared their OS, progression-free interval (PFI), disease-specific survival (DSS), and progression-free survival (PFS) outcomes. For PFI, the event is tumor-specific death, excluding other causes of death, which may be more relevant for cancer research. In contrast, PFS includes deaths from other causes without distinction. We utilized the "pheatmap" package to compare the differentially expressed genes between the high and low expression groups, followed by functional analysis of these genes using Gene Ontology (GO) and Kyoto Encyclopedia of Genes and Genomes (KEGG) pathways. We conducted GSEA using the "c2.cp.kegg.v7.4.symbols.gmt" gene set, and created a visualization of the top five KEGG pathways enriched in the high expression group.

To analyze the differences in clinical indicators between the high and low expression groups, we utilized "limma" and "ComplexHeatmap" and performed both univariate and multivariate COX analyses to determine the prognostic risk factors. We used the "ggplot2", "ggpubr", "ggExtra", "circlize", and "corrplot" packages to analyze and visualize the genes co-expressed with *SIGLEC9*. Using the "estimate" and "reshape2" packages, we assessed the TME and obtain StromalScore, ImmuneScore, and ESTIMATEScore, then compared the resulting gene expression differences and created visualizations. We used CIBERSORT to calculate immune cell infiltration scores for each sample, compared the expression levels of immune cells between groups with high and low *SIGLEC9* expression, and examined the potential correlation between immune cell expression and *SIGLEC9* gene expression. We planned to retrieve immune checkpoint genes and examined how they related to *SIGLEC9* gene expression. Additionally, we downloaded immunotherapy scoring files from The Cancer Immunome Atlas (TCIA, https://tcia.at/) to investigate potential disparities in *SIGLEC9* expression in the context of immunotherapy.

TIMER database

The TIMER database is a comprehensive platform designed for the systematic investigation of immune infiltration in various cancer types. It can be accessed at https://cistrome.shinyapps.io/timer/ and was last accessed on 16 Jan 2024. The database utilizes the TIMER deconvolution method to determine the presence of six distinct immune cell types and present the results through high-quality graphics. This allows for a comprehensive analysis of tumor immunology, clinical traits, and genomic properties [24]. We Examined the immune cell infiltration in SKCM, including B cells, CD8 + T cells, CD4 + T cells, macrophages, neutrophils, and dendritic cells, using the TIMER database to explore the relationship between *SIGLEC9* expression and immune cell infiltration.

Examining the expression of SIGLEC9 in different cell subpopulations of normal skin and SKCM at the single-cell level

We used the Human Protein Atlas (HPA) [25] at https://www.proteinatlas.org/ (accessed on 16 Jan 2024) to investigate the relationship between *SIGLEC9* expression and the single-cell microenvironment in normal skin. The TISCH database (http://tisch.comp-genomics.org/, accessed on 16 Jan 2024) is a scRNA-seq database that specifically focuses on the TME, compiling single-cell transcriptome data from high-quality tumor datasets [26]. At the single-cell level, TISCH provides detailed cell type annotation, enabling the investigation of the TME across various cancer types and the investigation of *SIGLEC9* expression in cell subpopulations within the SKCM TME. Additionally, the HPA database was utilized to investigate the protein expression of SIGLEC9 in both normal skin tissues and SKCM patients.

Results

High levels of SIGLEC9 expression are observed in SKCM, and its upregulation is linked to improved patient prognosis

Our analysis using the GEPIA2 database indicated that the expression of *SIGLEC9* was significantly higher in SKCM tumor tissue compared to normal skin tissue ($P < 0.05$, Fig. 1A). Specifically, differences in *SIGLEC9* expression were observed across different stages, with gradual increases from Stage II, III, and IV, but still lower than in Stage I, with significant differences ($F = 5.95$, $Pr = 0.000117 < 0.05$, Fig. 1B). Subsequent Kaplan–Meier survival analysis revealed that patients with high expression of the *SIGLEC9* gene had a relatively better OS ($P = 0.007 < 0.05$, Fig. 1C), however, DFS did not exhibit any statistically significant distinctions ($P = 0.22 > 0.05$, Fig. 1D). The Ualcan database also divided samples into UCP2 high expression group (with TPM value higher than the upper quartile of UCP2 expression) and low/medium expression group (with TPM value lower than the upper quartile of UCP2 expression), and found that high expression of UCP2 was associated with better prognosis ($P = 0.0018 < 0.05$, Fig. 1E). The SKCM data downloaded from the TCGA database were also divided into high and low expression groups based on the median value of *SIGLEC9* expression. Patients with high expression of *SIGLEC9* had better OS ($P < 0.001$), PFI ($P = 0.028$), and DSS ($P < 0.001$), but there was no significant difference in PFS ($P = 0.061 > 0.05$) (Fig. 1F-I). In addition, we observed a light brown staining of the SIGLEC9 protein in normal skin tissue, whereas in SKCM tissue, a dark brown staining was detected (Fig. 2). We discovered that the SIGLEC9 protein has a complex three-dimensional structure (Fig. 3A), and that the *SIGLEC9* gene has the highest mutation frequency in SKCM, reaching 5.41% (Fig. 3B). These mutations primarily affect the Immunoglobulin V-set domain (V-set), Immunoglobulin domain (151–216) (Ig-3), and Immunoglobulin domain (260–335) (Ig-3) regions (Fig. 3C).

Examining the correlation between clinical indicators and SIGLEC9 expression in patients through statistical analysis

Univariate and multivariate Cox regression analyses demonstrated that *SIGLEC9* is a protective factor for the prognosis of SKCM patients, with hazard ratio (HR) values of 0.582 (95% confidence interval [CI]

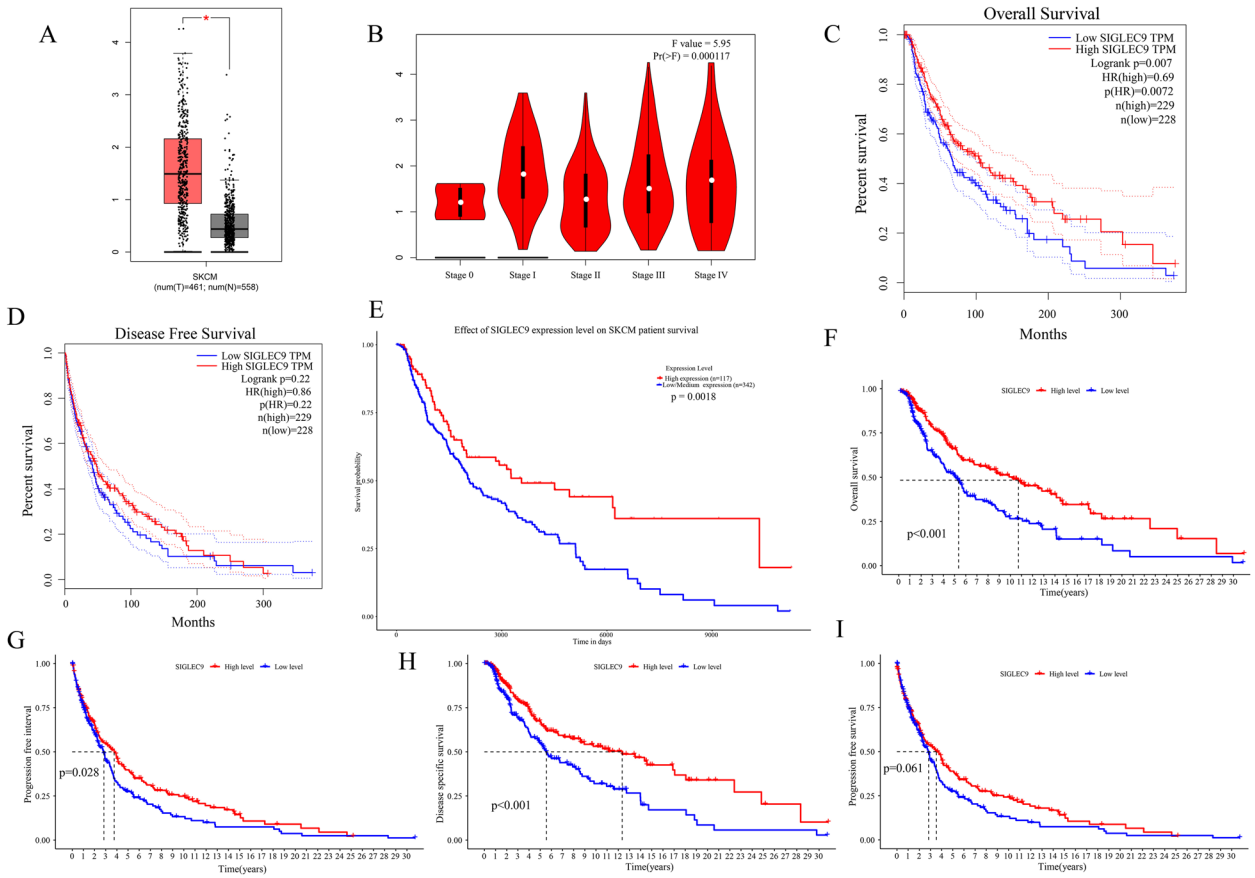

Fig. 1 Exploring the significance of *SIGLEC9* expression in SKCM and its implications for prognosis. **A** Examining the expression characteristics of both normal and cancerous SKCM tissues through GEPIA2 analysis (* $P<0.05$). **B** The expression patterns of *SIGLEC9* across different stages, as depicted in GEPIA2. **C-D** Analyzing the impact of high and low *SIGLEC9* expression levels on SKCM patient OS and DFS using data from the GEPIA2 database. **E** Analyzing the impact of high and low *SIGLEC9* expression levels on SKCM patient and OS using data from the Ualcan database. **F-I** Using TCGA data and Kaplan–Meier survival curves to explore the relationship between *SIGLEC9* expression levels and OS, PFI, DSS, and PFS in SKCM

0.446–0.761, $P<0.001$) and 0.644 (95% CI 0.493–0.840, $P=0.001$), respectively (Fig. 4A-B). Investigating the correlation between *SIGLEC9* expression and clinical indicators in SKCM revealed a statistically significant association between higher expression levels of *SIGLEC9* and age ≤ 65 years ($P=0.016<0.05$) and T1-2 stage tumors ($P=0.00017<0.05$). However, *SIGLEC9* expression showed no significant difference among SKCM patients with different genders ($P=0.24$), stages (stage1-2 vs. stage3-4, $P=0.34$), lymph node status (N0 vs. N1, $P=0.44$), or metastasis status (M0 vs. M1, $P=0.54$) (Fig. 4C). After combining clinical data and *SIGLEC9* expression, we developed a predictive nomogram model for the prognosis of SKCM patients at 1, 3, and 5 years (Fig. 5A). Calibration analysis revealed that the predicted probabilities and observed probabilities of patient outcomes at 1, 3, and 5 years were well-matched, indicating that our nomogram model could be used to predict the prognosis of SKCM patients (Fig. 5B). Subsequently, we performed a subgroup analysis and observed that high *SIGLEC9* expression was associated with a better OS than low expression in both female ($P=0.032$) and male patients ($P<0.001$, Fig. 5C). As there were relatively few patients over 65 years old and in the M1 stage, OS analysis was not conducted. We found that high *SIGLEC9* expression was associated with a better prognosis in patients aged ≥ 65 years ($P<0.001$, Fig. 5D) and in the M0 stage ($P<0.001$, Fig. 5E*)*. Similarly, we found that high *SIGLEC9* expression was associated with better OS in the N0 ($P=0.014$) and N1-3 subgroups ($P=0.003$, Fig. 5F), Stage 1–2 ($P=0.013$) and Stage 3–4 subgroups ($P=0.002$, Fig. 5G), and T1-2($P=0.008$) and T3-4 subgroups ($P=0.009$, Fig. 5H).

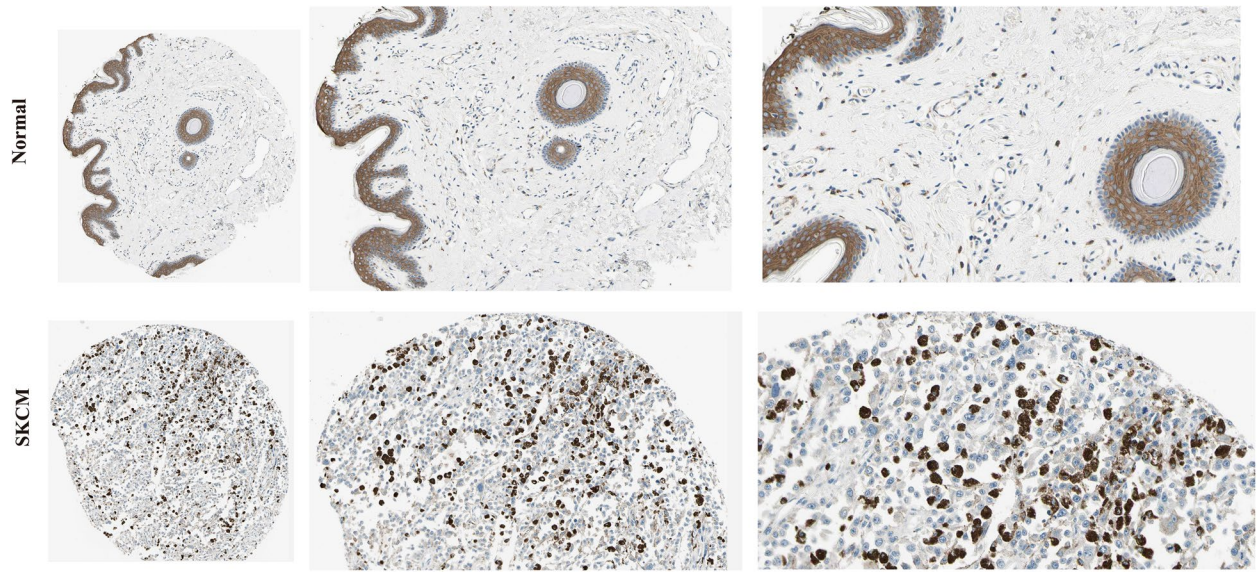

Fig. 2 The expression of the SIGLEC9 protein in normal skin and SKCM tissue, as shown by scale bars, with lengths of 100 μm, 50 μm, and 25 μm from left to right

Analysis of genes co-expressed with SIGLEC9 in SKCM

Based on our analysis, we have identified genes that show both positive and negative regulation with *SIGLEC9* (Fig. 6A). Specifically, the genes that exhibiting negative regulation include ADGRA3, MTURN, CLBA1, SNHG8, and ESRP1. The circular plot reveals that genes that exhibiting positive regulation with *SIGLEC9* are predominantly HAVCR2 (R = 0.92, $P < 0.001$), LAIR1 (R = 0.93, $P < 0.001$), LILRB4 (R = 0.91, $P < 0.001$), LRRC25 (R = 0.94, $P < 0.001$), PILRA (R = 0.92, $P < 0.001$), and SIGLEC7 (R = 0.92, $P < 0.001$) (Fig. 6B-G).

Functional analysis of differentially expressed genes in SIGLEC9-based groups

After dividing SKCM patients into high and low expression groups based on the median expression level of *SIGLEC9*, we identified genes with significantly different expression levels between the two groups (Fig. 7A). Furthermore, GSEA analysis showed that immune-related pathways were enriched in the high expression group of *SIGLEC9*, with the Chemokine signaling pathway, Cytokine-cytokine receptor interaction, Hematopoietic cell lineage, and primary immunodeficiency being the most significant pathways (Fig. 7B). GO analysis revealed that the high expression group of *SIGLEC9* was closely associated with immune-related biological processes, cellular components, and molecular functions (Fig. 7C). The KEGG analysis showed that the majority of differentially expressed genes were involved in immune-related pathways, including Cytokine-cytokine receptor interaction, Chemokine signaling pathway, Cell adhesion molecules, Antigen processing and presentation, Natural killer cell mediated cytotoxicity, and Th17 cell differentiation (Fig. 7D).

Verification of the close association between SIGLEC9 and TME immunity using bulk RNA

The computation of immune cell abundance in the TMEt indicated a higher score for T cells CD8, T cells CD4 memory activated, T cells regulatory (Tregs), NK cells resting, Monocyte, and Macrophages M1 in the high *SIGLEC9* expression group, whereas Macrophages M0 had a lower score in the same group (all $P < 0.05$, Fig. 8A). Subsequently, the investigation into the correlation between *SIGLEC9* and immune cells revealed that *SIGLEC9* expression levels were positively correlated with T cells CD8 (R = 0.4, $P = 1.9E\text{-}10$), T cells CD4 memory activated (R = 0.32, $P = 4E\text{-}07$), Monocyte (R = 0.27, $P = 3.1E\text{-}05$), Macrophages M1 (R = 0.2, $P = 0.0017$), and Dendritic cells resting (R = 0.17, $P = 0.01$), and negatively correlated with Macrophages M0 (R = -0.32, $P = 7.5E\text{-}07$) (Fig. 8B-C). Following validation using the TIMER database, positive correlations were observed between *SIGLEC9* expression and various immune cells, including B cells (R = 0.249, $P = 9.84E\text{-}08$), CD8 + T cells (R = 0.509, $P = 2.76E\text{-}30$), CD4 + T cells (R = 0.334, $P = 4.57E\text{-}13$), macrophages (R = 0.628, $P = 5.43E\text{-}51$), neutrophils ($R = 0.68$, P = 1.11E-62), and dendritic cells (R = 0.763, $P = 3.45E\text{-}86$) (all $P < 0.001$, Fig. 8D).

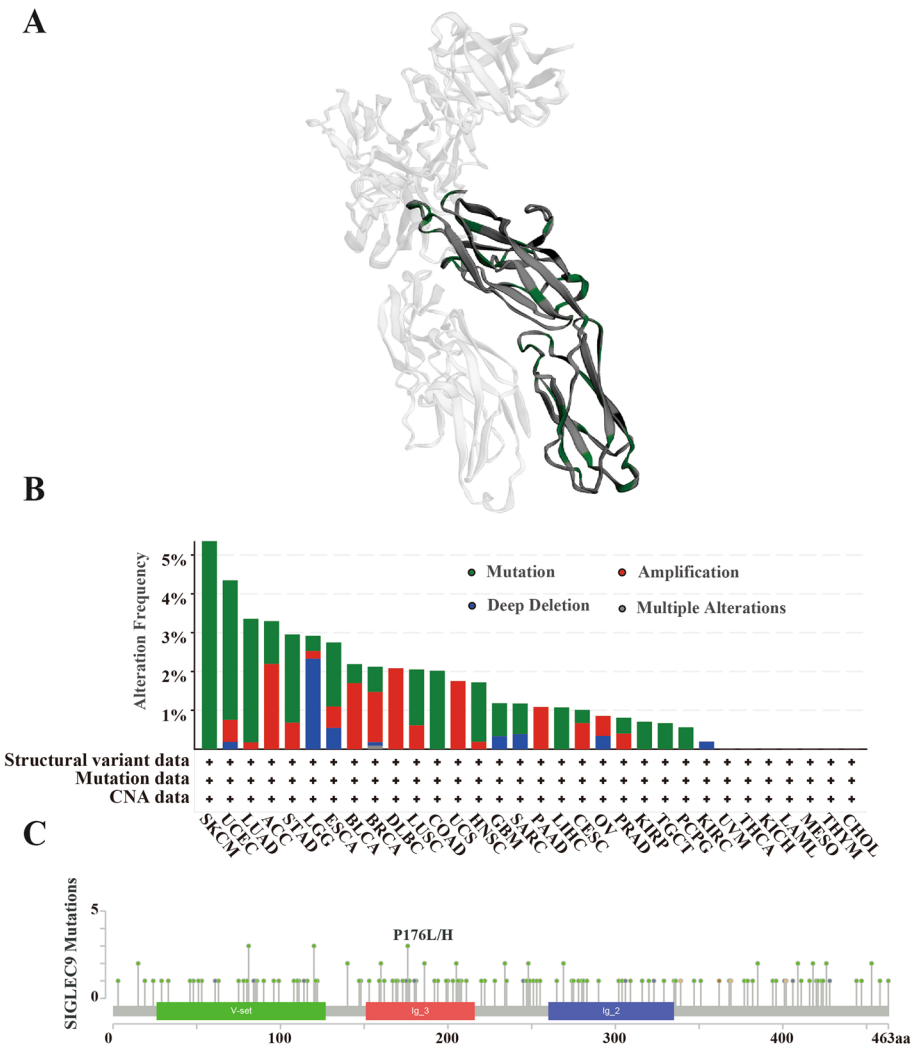

Fig. 3 The three-dimensional structure of SIGLEC9 protein and the status of gene mutations. **A** Three-dimensional structure of the SIGLEC9 protein. **B** Pan-cancer analysis of mutations in the *SIGLEC9* gene. **C** Location of mutations in *SIGLEC9*

Correlation analysis of SIGLEC9 with immune checkpoints and immune therapy in SKCM

After analyzing the data, a significant positive correlation was found between immune checkpoint gene expression and *SIGLEC9*. The strongest correlations were observed with LAIR1 (R = 0.928), HAVCR2 (R = 0.918), CD86 (R = 0.895), LGALS9 (R = 0.748), PDCD1LG2 (R = 0.743), LAG3 (R = 0.734), TNFRSF9 (R = 0.728), CD80 (R = 0.726), PDCD1 (R = 0.716), TIGIT (R = 0.713), CD27 (R = 0.702), and CTLA4 (R = 0.406) (all $P < 0.001$, Fig. 9A). Upon analysis of the immune therapy data, it was discovered that the difference in immune therapy between high and low *SIGLEC9* expression groups in IPS_CTLA4_Neg_PD1_Neg ($P = 0.2$) and IPS_CTLA4_Pos_PD1_Neg ($P = 0.31$) was not significant. However, a difference in immune therapy was observed between high and low *SIGLEC9* expression groups in IPS_CTLA4_Neg_PD1_Pos ($P = 1.4E\text{-}13$) and IPS_CTLA4_Pos_PD1_Pos ($P < 2.22E\text{-}16$) groups. Additionally, patients with high *SIGLEC9* expression demonstrated higher immune scores (Fig. 9B). Upon analyzing score differences in the TME, it was discovered that patients with high expression of *SIGLEC9* had higher StromalScore, ImmuneScore, and ESTIMATEScore compared to those with low expression (*** $P < 0.001$, Fig. 9C).

The single-cell RNA transcriptome analysis has verified that immune cells within normal skin and SKCM exhibit primarily high expression of SIGLEC9

At the single-cell level, our ongoing investigation is focused on examining the correlation between immune cells and the expression of *SIGLEC9*. The predominant expression of *SIGLEC9* in Langerhans cells located within certain subpopulations of cells in normal skin

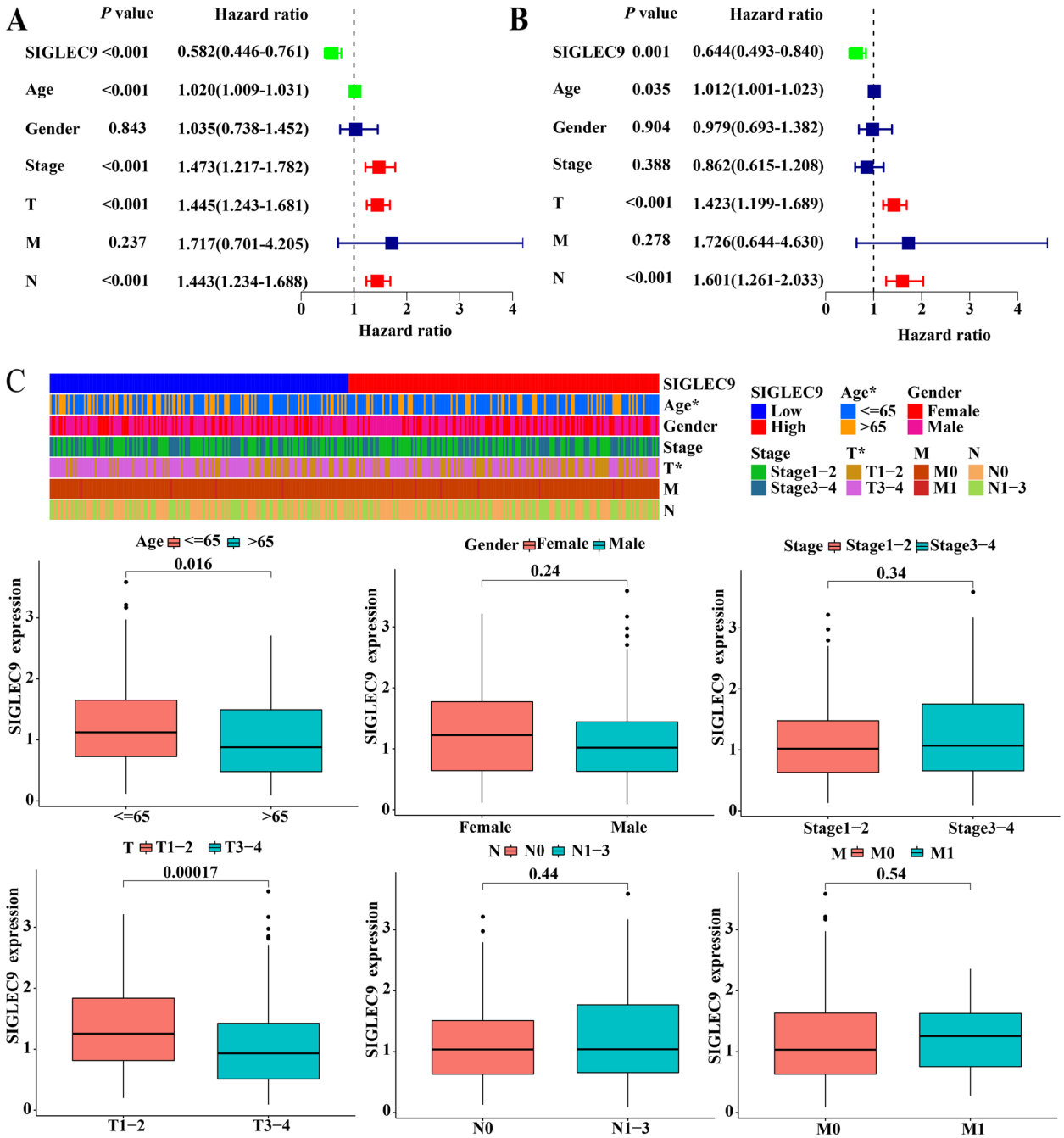

Fig. 4 *SIGLEC9* expression and its association with clinical parameters in patients. **A** Univariate Cox analysis evaluating prognostic factors in SKCM. **B** Multivariate Cox analysis evaluating factors in SKCM. **(C)***SIGLEC9* expression in relation to clinical indicators

(See figure on next page.)

Fig. 5 Prognostic analysis of SKCM patients. **A** Nomogram for predicting prognosis. **B** Calibration curves for the Nomogram. **C** OS curves for female and male patients with high and low expression of *SIGLEC9*. **D** OS curves for ≥ 65 years with high and low expression of *SIGLEC9*. **E** OS curves for M0 patients with high and low expression of *SIGLEC9*. **F** OS curves for N0 and N1-3 patients with high and low expression of *SIGLEC9*. **G** OS curves for Stage 1–2 and Stage 3–4 patients with high and low expression of *SIGLEC9*. **H** OS curves for T1-2 and T3-4 patients with high and low expression of *SIGLEC9*

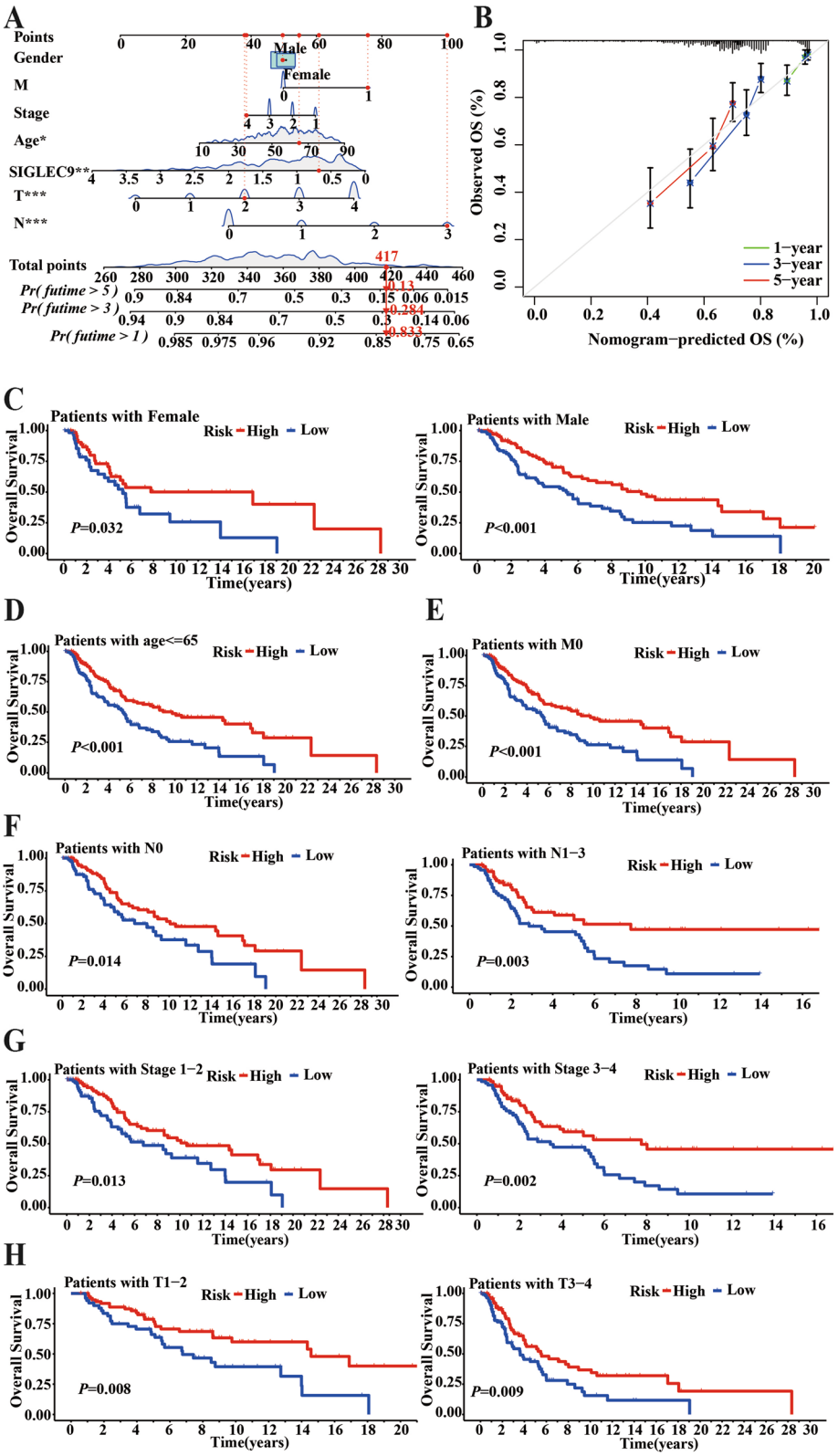

Fig. 5 (See legend on previous page.)

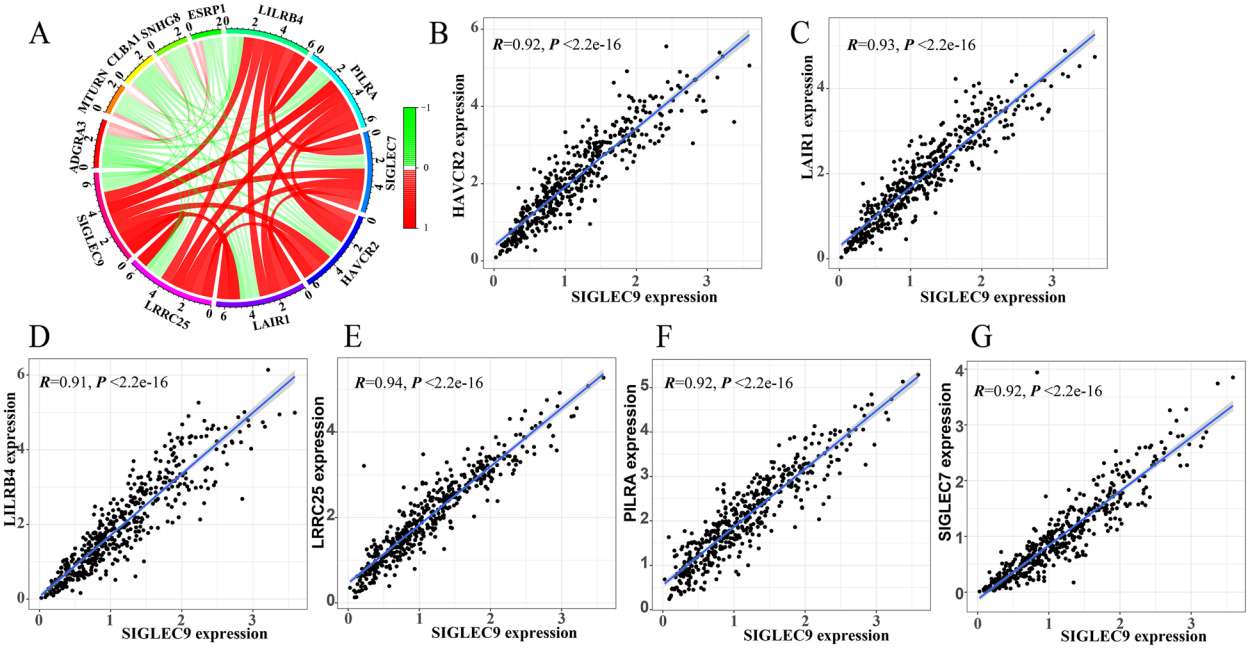

Fig. 6 Co-expression analysis of genes with *SIGLEC9*. **A** Circular visualization tool for analyzing co-expressed genes. **B-G** Scatter plot visualizing the positive correlation between *SIGLEC9* and its co-expressed genes

tissue was discovered through HPA analysis, indicating its involvement in the development of the immune microenvironment of normal skin (Fig. 10). In the following section, we will delve into the expression pattern of the *SIGLEC9* subpopulation in the single-cell SKCM TME. Our analysis of the TISCH database has revealed that *SIGLEC9* expression is predominantly high in monocyte macrophages across the GSE115978, GSE120575, GSE123139, GSE139249, and GSE72056 datasets. Interestingly, the GSE123139 and GSE139249 databases also exhibit a marked upregulation of *SIGLEC9* expression in dendritic cells, as highlighted in Fig. 11.

Subgroup analysis of SIGLEC9

Using the "ConsensusClusterPlus" R package, we categorized SKCM patients into two clusters (C1 and C2, Fig. 12A). Our analysis of patient survival indicated that C2 had significantly different outcomes compared to C1 in terms of OS ($P<0.001$, Fig. 12B), DSS ($P<0.001$, Fig. 12C), and PFI ($P=0.018$, Fig. 12D). Subgroup analysis showed that both male ($P<0.001$) and female ($P=0.025$) patients in the C2 had better prognoses than those in the C1 (Fig. 13A). However, due to the relatively small number of patients over 65 years old and those in the M1 stage, survival analysis was not conducted. In the study, it was discovered that the C2 had a better prognosis for patients aged ≥ 65 ($P<0.001$, Fig. 13B) and in M0 stage ($P<0.001$, Fig. 13C). Additionally, subgroup analysis of N0 ($P<0.001$) and N1-3 ($P=0.007$, Fig. 13D), Stage 1–2 ($P<0.001$) and Stage 3–4 ($P=0.003$, Fig. 13E), T1-2 ($P=0.002$) and T3-4 ($P=0.018$, Fig. 13F) also showed that patients in the C2 had significantly better prognoses than those in the C1. Furthermore, an analysis was carried out on the relationship between clustering and immunity. It was found that there were extensive differences in immune checkpoints (Fig. 14A) and immune cells infiltrating the TME (Fig. 14B) between the C1 and C2 clusters, with the C2 having significantly higher levels than the C1.

Discussion

Our study has identified high levels of *SIGLEC9* expression in SKCM patients, with those exhibiting high expression displaying superior OS, PFI, and DSS compared to those with low expression, although no advantage was observed in DFS and PFS. Additionally, we have found that *SIGLEC9* is closely associated with immune infiltration in the SKCM TME, and functional analysis has revealed a strong correlation between high levels of *SIGLEC9* expression and immune-related biological functions. Furthermore, our findings at the single-cell level have confirmed that *SIGLEC9* is not only highly expressed in immune cells of normal skin but also present in certain immune cells of the SKCM single-cell subpopulation, demonstrating significant high expression. Our study thus concludes that *SIGLEC9* is closely

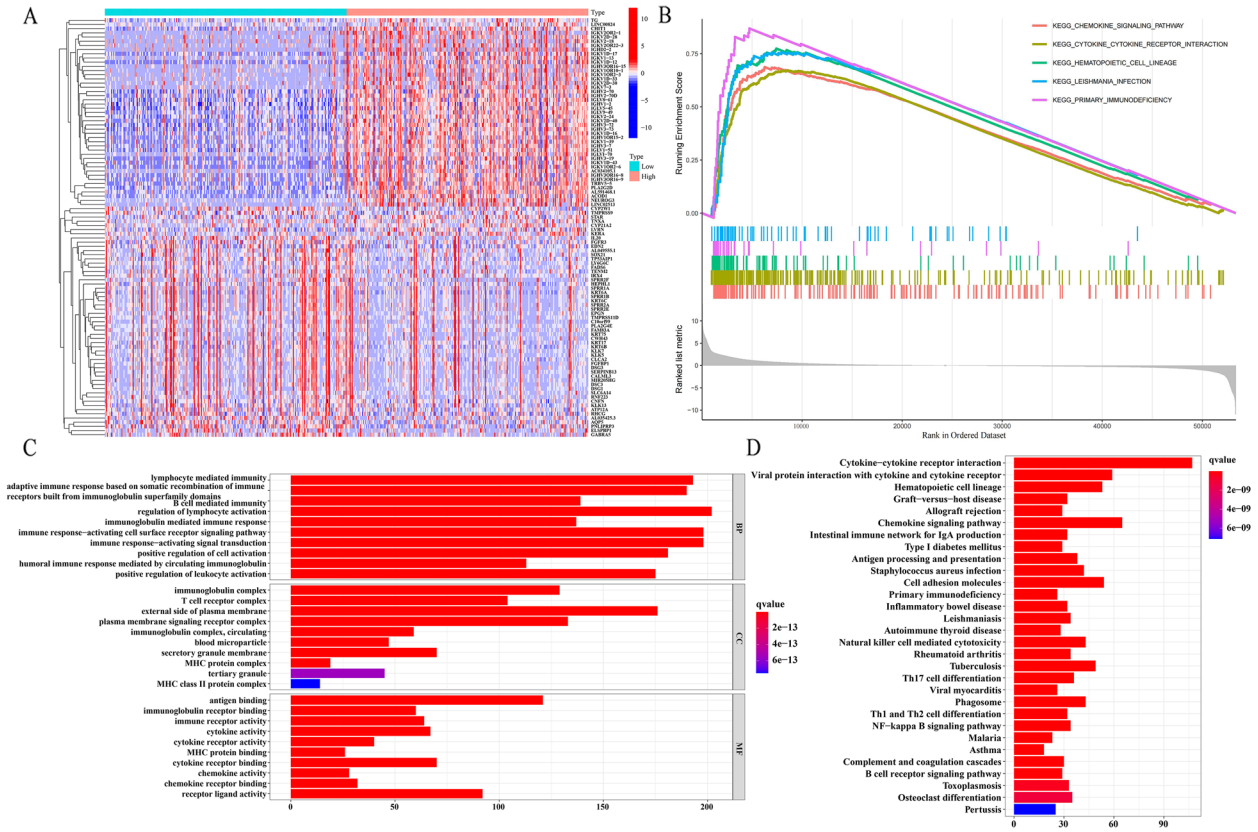

Fig. 7 Analysis of gene expression differences and functions between *SIGLEC9* groups. **A** Visualization of gene expression differences between high and low *SIGLEC9* expression groups using a heat-map. **B** Functional analysis of differentially expressed genes using GSEA. **C** Functional analysis of differentially expressed genes using GO. **D** Functional analysis of differentially expressed genes using KEGG

linked to the TME of SKCM. We divided SKCM patients into C1 and C2 clusters, where C2 had higher levels of immune checkpoints and immune cell infiltration, and showed significantly different outcomes compared to C1 in terms of OS, DSS, and PFI.

In the immune microenvironment of SKCM, various types of TILs are present, including macrophages, dendritic cells, T cells, B cells, and natural killer cells [27]. These TILs play crucial roles in immune regulation and tumor progression within the local microenvironment of SKCM, making them a potential targets for SKCM treatment [1, 28]. This study also discovered a significant positive association between *SIGLEC9* expression and several immune cell types, including CD8 + T cells, CD4 + T cells, T Tregs, resting NK cells, Monocytes, and M1 Macrophages, in the SKCM TME. Based on our previous findings showing that high *SIGLEC9* expression is associated with a better clinical prognosis, we hypothesize that *SIGLEC9*-positive patients have a TME rich in immune responses that inhibit tumors progression. This suggests that *SIGLEC9* plays a crucial regulatory role in the SKCM TME. Targeting *SIGLEC9* in the TME may enhance the tumor immune response and improve patient prognosis, making it a promising therapeutic target for SKCM.

Currently, it has been shown through in vitro experiments that recombinant *SIGLEC9* has the potential to treat SKCM by inducing cytotoxic effects and promoting the apoptosis of tumor cells. These findings underscore the therapeutic benefits of recombinant *SIGLEC9* in SKCM [20, 21]. *SIGLEC9* has been shown to initiate the degradation of FAK and related molecules, thereby regulating cancer cell adhesion dynamics. This mechanism may enable cancer cells to evade immune surveillance via *SIGLEC9* [18, 29, 30]. Additionally, studies have indicated that the interaction between *MUC1* and *SIGLEC9* on monocytes/macrophages within the tumor can induce the TAM phenotype. This phenotype is characterized by the suppression of CD8 + T cell proliferation and an increase in the expression of scavenger receptor *CD163*, mannose receptor *CD206*, and immune checkpoint ligand PD-L1, thereby influencing the tumor's immune microenvironment [31].

However, when *SIGLEC9* binds to activating antibodies, it enhances the immune response. As an immune

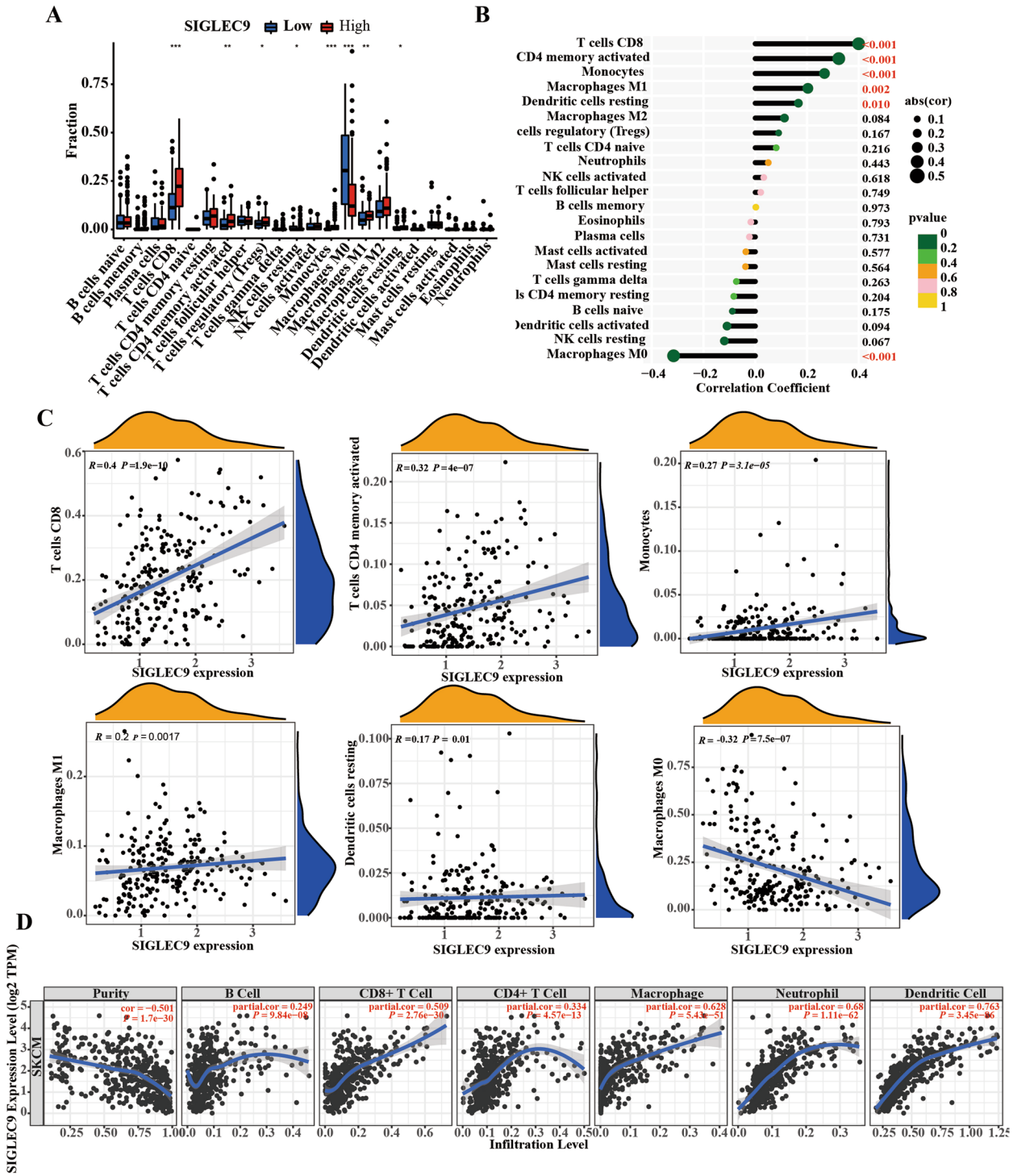

Fig. 8 Investigation of the immune correlation between *SIGLEC9* and the TME. **A** Analysis of the relative abundance of immune cells between the high and low *SIGLEC9* expression groups. (* $P < 0.05$, ** $P < 0.01$, *** $P < 0.001$). **B** Correlation analysis of immune cells with *SIGLEC9* expression. **C** Validation of the association between *SIGLEC9* expression and immune cells using the TIMER database

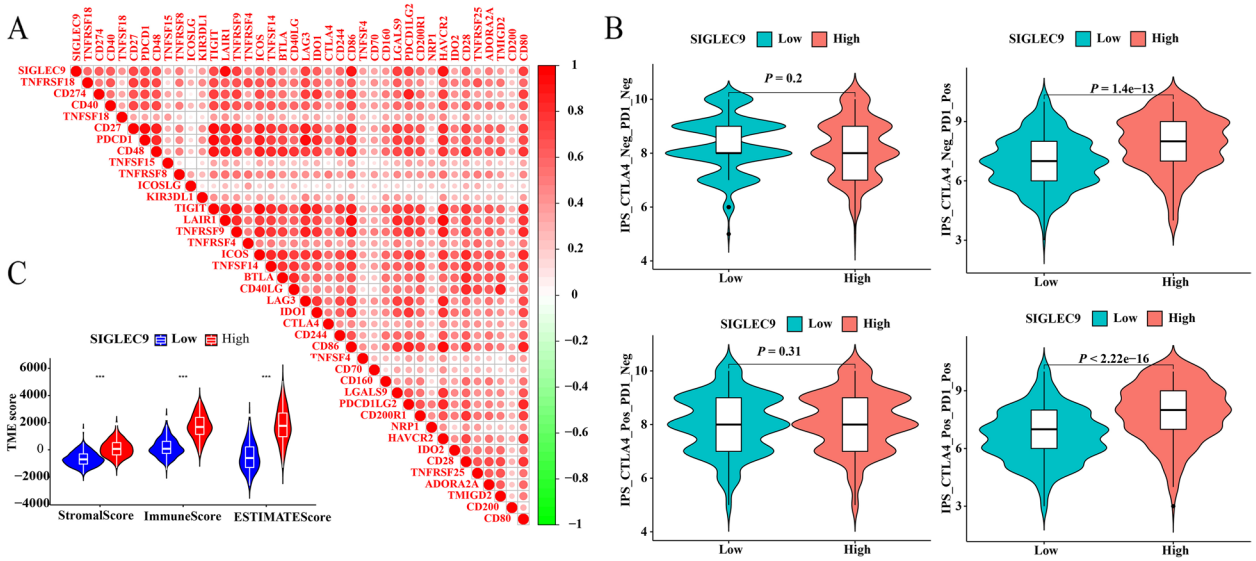

Fig. 9 Analysis of *SIGLEC9* with immune checkpoints and immune therapy. **A** The heatmap illustrates the correlation between immune checkpoint genes and *SIGLEC9* expression, where darker shades of red indicate a stronger correlation. **B** Analysis of differences in immune therapy among patients with different levels of *SIGLEC9* expression. **C** Analysis of differences in StromalScore, ImmuneScore, and ESTIMATEScore between high and low *SIGLEC9* expression groups in the TME (*** $P < 0.001$)

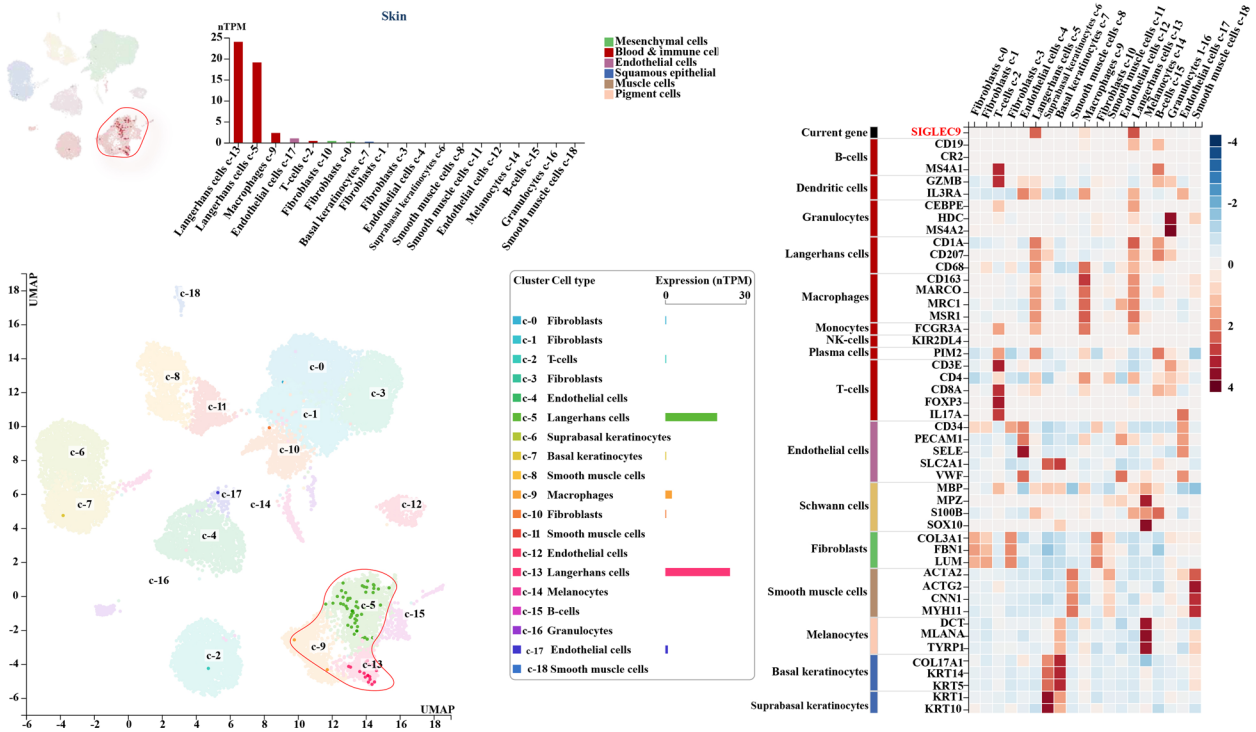

Fig. 10 The expression profile of *SIGLEC9* in various subpopulations of single cells present in the normal skin was be explored

checkpoint and inhibitory receptor, *SIGLEC9* holds promise for developing antibodies that target various immune regulations in cancer immunotherapy [16]. Recent research has shown that the activation of LINC01004-SPI1 axis by tumor-associated macrophages in esophageal squamous cell carcinoma can induce the transcriptional activation of *SIGLEC9*, leading to immunosuppression and radioresistance [32]. Conversely,

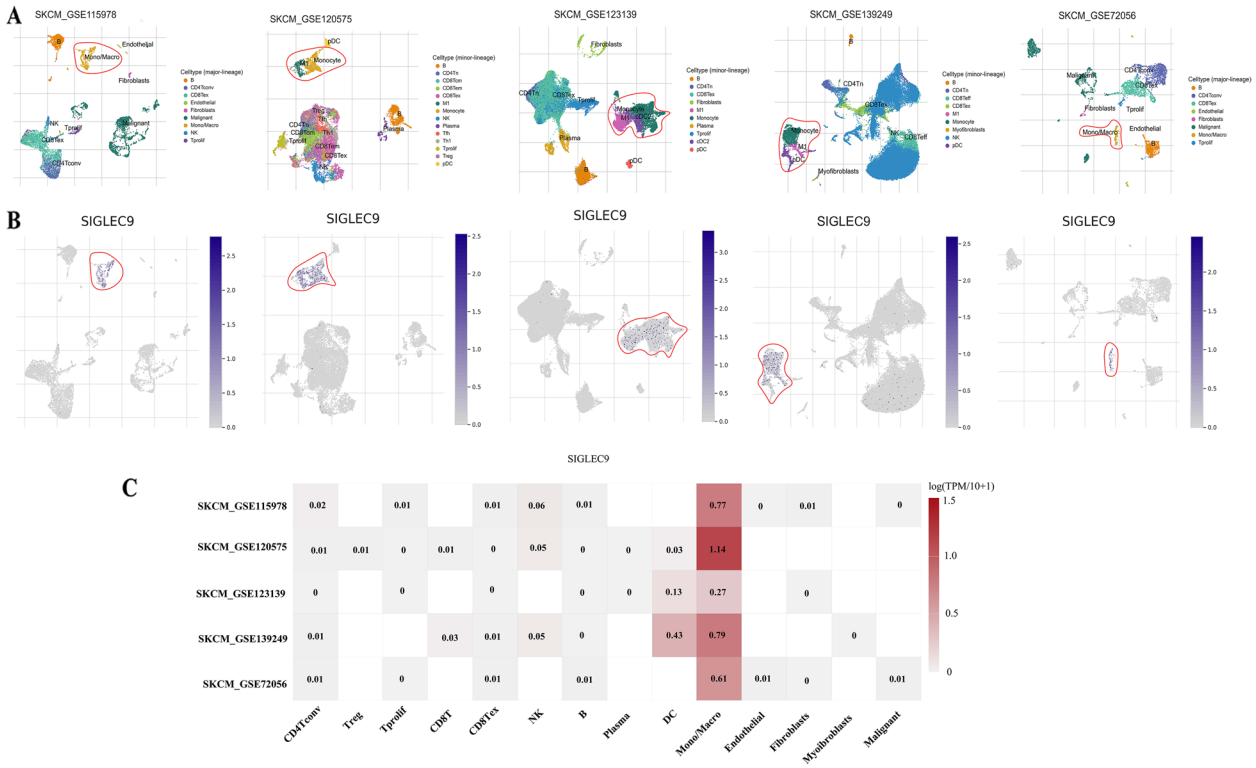

Fig. 11 The expression profile of *SIGLEC9* in various subpopulations of single cells present in SKCM was be explored

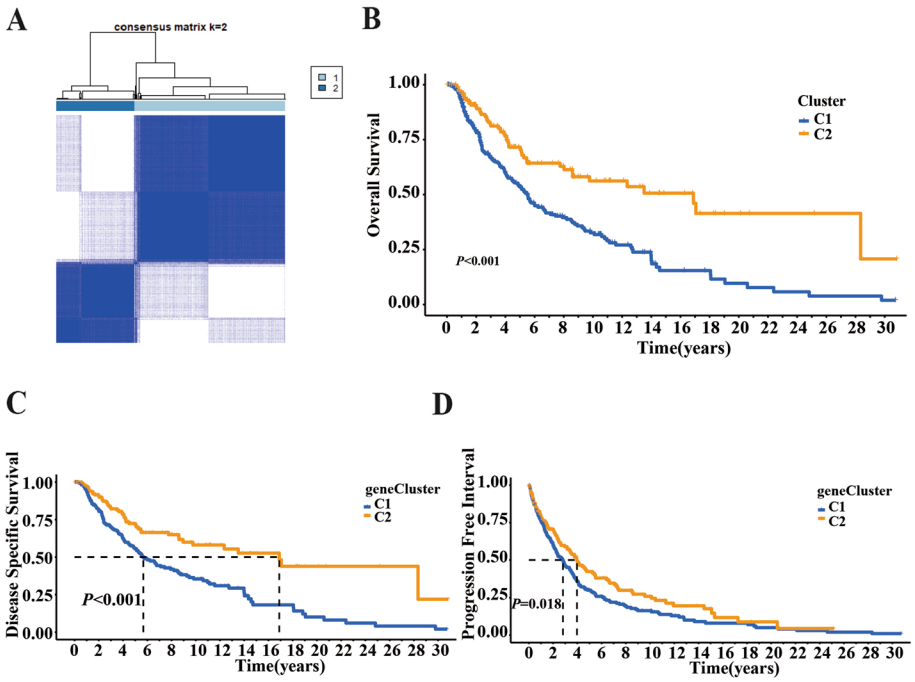

Fig. 12 Cluster analysis of *SIGLEC9*. **A** The consensus matrices of the clusters. **B** Kaplan–Meier survival curve of OS between C1 and C2. **C** Kaplan–Meier survival curve of DSS between C1 and C2. **D** Kaplan–Meier survival curve of PFI between C1 and C2

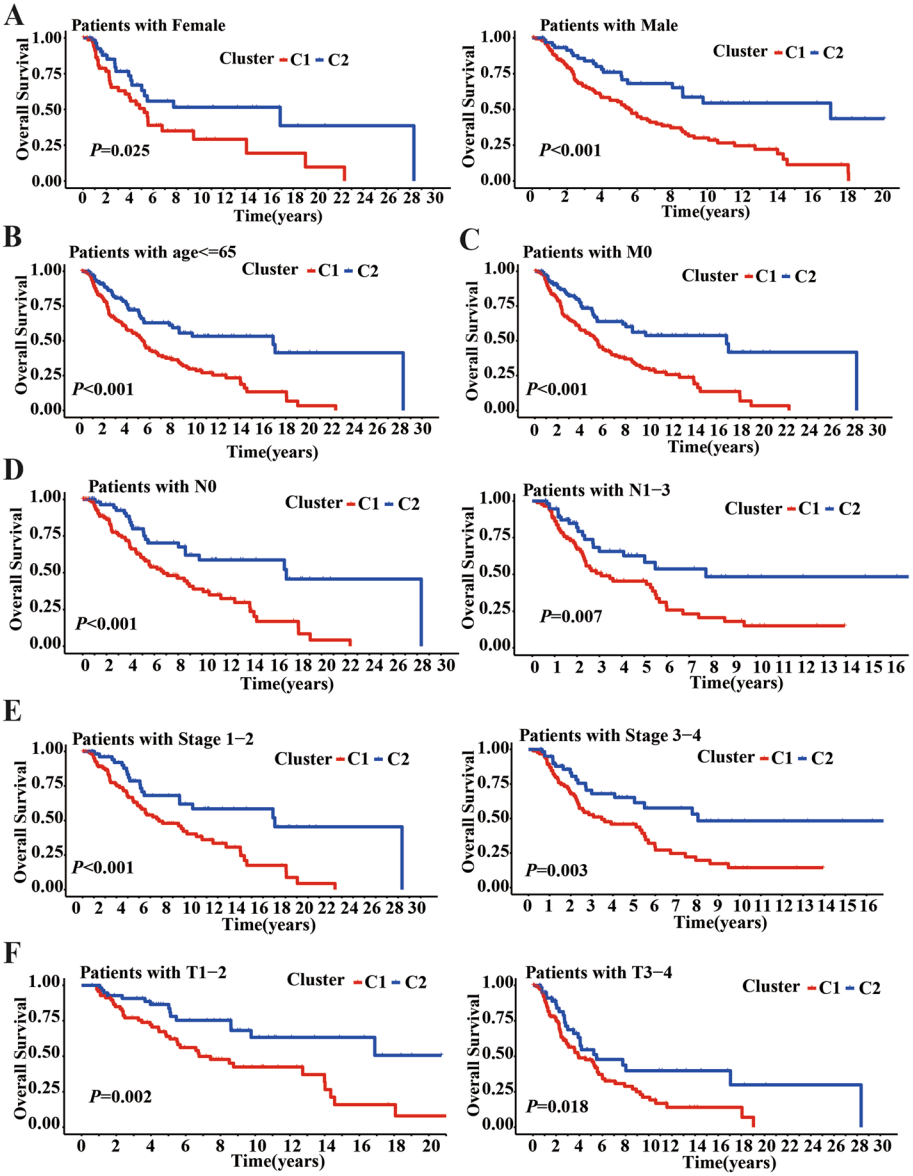

Fig. 13 Analysis of prognostic subgroups in SKCM. **A** OS curves for female and male patients in C1 and C2 clusters. **B** OS curves for age ≥ 65 years patients in C1 and C2 clusters. **C** OS curves for M0 patients in C1 and C2 clusters. **D** OS curves for N0 and N1-3 patients in C1 and C2 clusters. **E** OS curves for Stage 1–2 and Stage 3–4 patients in C1 and C2 clusters. **F** OS curves for T1-2 and T3-4 patients in C1 and C2 clusters

some experts have a different perspective, suggesting that individuals with high expression of *SIGLEC9* in glioma may have a worse prognosis than those with low expression. This is attributed to the ability of *SIGLEC9* to regulate myeloid-derived suppressor cells and neutrophils, enhance the expression of immune checkpoint genes, influence the TME, and promote tumor growth, metastasis, and resistance to glioblastoma therapies [17]. Targeting the SKCM Siglec-9 axis in SKCM may release the CD8 + T cell subset within the tumor and limit T cell activation within the TME [20] Moreover, a strong association was observed between *SIGLEC9* expression and immune checkpoints including *LAIR1*, *HAVCR2*, *CD86*, *LGALS9*, *PDCD1LG2*, *LAG3*, *TNFRSF9*, *PDCD1*, and *CTLA4*, among patients with high *SIGLEC9* expression. Additionally, these patients showed a more favorable response to immunotherapy targeting SKCM immune checkpoints.

Analyzing the TME of SKCM and the correlation and regulatory mechanisms of genes at the single-cell level is crucial for advancing the precision medicine [28, 33]. Therefore, this study examined the expression

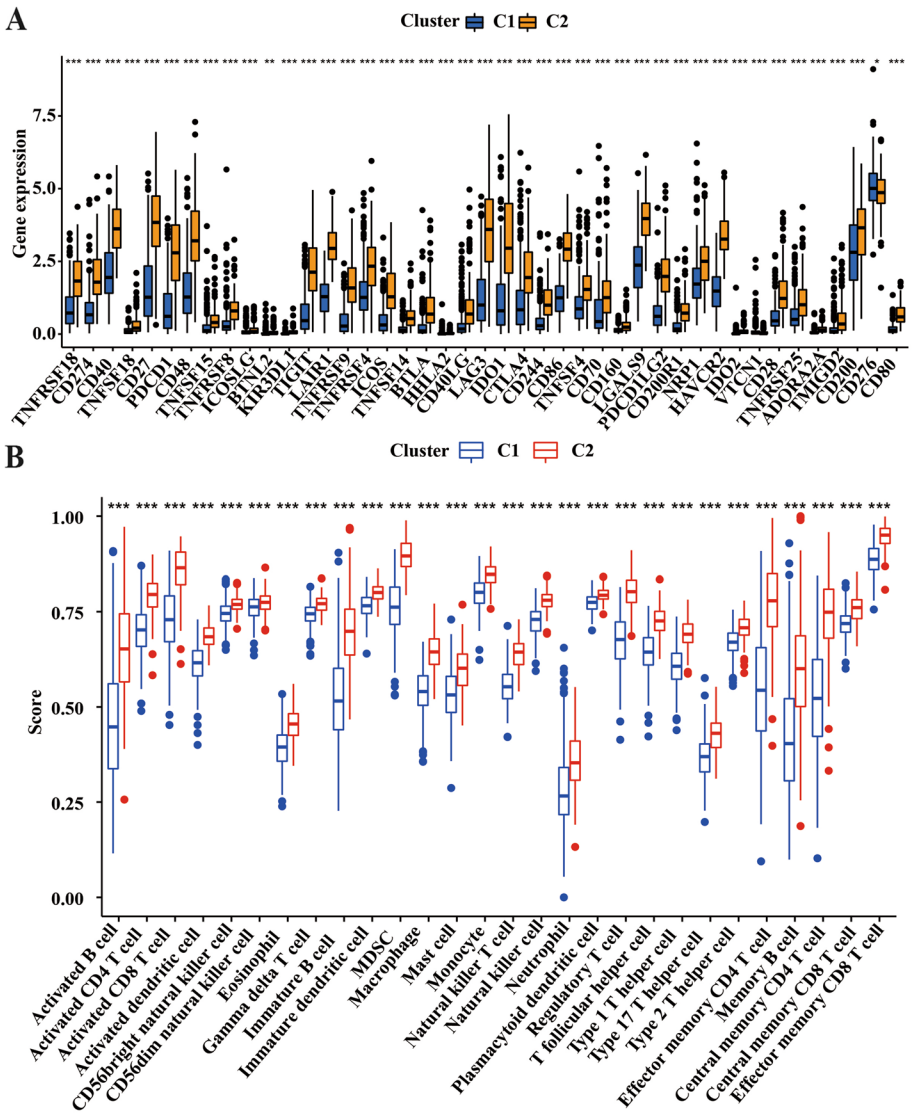

Fig. 14 The immune-related analysis of SKCM patient clustering. **A** Analysis of differential immune checkpoints between C1 and C2 clusters. (*$P < 0.05$, **$P < 0.01$, ***$P < 0.001$). **B** Analysis of differential immune cells infiltrating the TME between C1 and C2 clusters. (*$P < 0.05$, **$P < 0.01$, ***$P < 0.001$)

of the *SIGLEC9* gene in single cells from normal skin and found that it was predominantly highly expressed in Langhans immune cells, indicating that *SIGLEC9* mainly participates in the construction of the normal skin TME. In multiple SKCM single-cell libraries, *SIGLEC9* was primarily highly expressed in monocyte macrophages and dendritic cells of the TME, indicating that *SIGLEC9* may be an essential factor in maintaining and regulating the SKCM TME.

This study aims to design relevant experiments to validate the specific immune-related regulatory mechanism of *SIGLEC9* in the TME of SKCM. The research discovered that *SIGLEC9* is highly expressed in cancerous tissue and that SKCM patients with high expression have a better prognosis. By integrating multiple databases, the study confirmed that *SIGLEC9* plays an immune regulatory role in the TME at both the overall tissue transcriptome level and single-cell transcriptome level, providing a promising therapeutic target for SKCM immunotherapy.

Acknowledgements
Sincere appreciation to all scholars for contributing diverse public databases to advance scientific progress, enrich our research, and provide valuable references.

Authors' contributions
Peipei Yang, Yunhui Jiang and Rong Chen contributed to perform the experiments, analyze and interpret the data, prepare reagents, materials, analysis tools or data and write the paper. Junhan Yang performed the experiments, analyzed and interpreted the data, contributed reagents, materials, analysis tools or data. Mengting Liu and Xieping Huang analyzed and interpreted the data and performed the experiments. Ganglin Xu and Rui Hao conceived and designed the experiments and analyzed and interpreted the data. All authors commented on previous versions of the manuscript. All authors read and approved the final manuscript.

Funding
This work was supported by Guiding project for the Jingmen science and technology research and development plan (2024YDKY001).

Availability of data and materials
We obtained clinical and transcriptomic data on SKCM from the TCGA Database (https://portal.gdc.cancer.gov/).

Data availability
No datasets were generated or analysed during the current study.

Declarations

Ethics approval and consent to participate
The data was downloaded from public databases and did not require ethical approval. However, we followed the regulations set by the public databases.

Consent for publication
Consent for publication was obtained from the participants.

Competing interests
The authors declare no conflict of interest.

Received: 25 June 2024 Accepted: 12 August 2024
Published online: 17 August 2024

References

1. Lim SY, et al. The molecular and functional landscape of resistance to immune checkpoint blockade in melanoma. Nat Commun. 2023;14(1):1516.
2. Skudalski L, et al. Melanoma an update on systemic therapies. J Am Acad Dermatol. 2022;86(3):515–24.
3. Li J, et al. Single cell characterization of the cellular landscape of acral melanoma identifies novel targets for immunotherapy. Clin Cancer Res. 2022;28(10):2131–46.
4. Luke JJ, et al. Targeted agents and immunotherapies: optimizing outcomes in melanoma. Nat Rev Clin Oncol. 2017;14(8):463–82.
5. Ziogas DC, et al. Mechanisms of resistance to immune checkpoint inhibitors in melanoma: what we have to overcome? Cancer Treat Rev. 2023;113: 102499.
6. Lee AY, Brady MS. Neoadjuvant immunotherapy for melanoma. J Surg Oncol. 2021;123(3):782–8.
7. Brenner E, Röcken M. A commotion in the skin: developing melanoma immunotherapies. J Invest Dermatol. 2022;142(8):2055–60.
8. Sadeghi Rad H, et al. Understanding the tumor microenvironment for effective immunotherapy. Med Res Rev. 2021;41(3):1474–98.
9. de Visser KE, Joyce JA. The evolving tumor microenvironment: from cancer initiation to metastatic outgrowth. Cancer Cell. 2023;41(3):374–403.
10. Zhou H, et al. Functions and clinical significance of mechanical tumor microenvironment: cancer cell sensing, mechanobiology and metastasis. Cancer Commun (Lond). 2022;42(5):374–400.
11. Goliwas KF, et al. Moving immune therapy forward targeting TME. Physiol Rev. 2021;101(2):417–25.
12. Tiwari A, et al. Tumor microenvironment: barrier or opportunity towards effective cancer therapy. J Biomed Sci. 2022;29(1):83.
13. Rabinovich GA, Conejo-García JR. Shaping the immune landscape in cancer by galectin-driven regulatory pathways. J Mol Biol. 2016;428(16):3266–81.
14. Bochner BS, Zimmermann N. Role of siglecs and related glycan-binding proteins in immune responses and immunoregulation. J Allergy Clin Immunol. 2015;135(3):598–608.
15. Stanczak MA, et al. Self-associated molecular patterns mediate cancer immune evasion by engaging Siglecs on T cells. J Clin Invest. 2018;128(11):4912–23.
16. Wang JHS, et al. Development of effective siglec-9 antibodies against cancer. Curr Oncol Rep. 2023;25(1):41–9.
17. Xu H, et al. High expression levels of SIGLEC9 indicate poor outcomes of glioma and correlate with immune cell infiltration. Front Oncol. 2022;12: 878849.
18. Rodriguez E, et al. Sialic acids in pancreatic cancer cells drive tumour-associated macrophage differentiation via the Siglec receptors Siglec-7 and Siglec-9. Nat Commun. 2021;12(1):1270.
19. Tao L, et al. Reduced Siglec-7 expression on NK cells predicts NK cell dysfunction in primary hepatocellular carcinoma. Clin Exp Immunol. 2020;201(2):161–70.
20. Haas Q, et al. Siglec-9 regulates an effector memory CD8+ T-cell subset that congregates in the melanoma tumor microenvironment. Cancer Immunol Res. 2019;7(5):707–18.
21. Wiersma VR, et al. The glycan-binding protein galectin-9 has direct apoptotic activity toward melanoma cells. J Invest Dermatol. 2012;132(9):2302–5.
22. Tang Z, et al. GEPIA2: an enhanced web server for large-scale expression profiling and interactive analysis. Nucleic Acids Res. 2019;47(W1):W556–60.
23. Chandrashekar DS, et al. UALCAN: a portal for facilitating tumor subgroup gene expression and survival analyses. Neoplasia. 2017;19(8):649–58.
24. Li T, et al. TIMER: AWeb server for comprehensive analysis of tumor-infiltrating immune cells. Cancer Res. 2017;77(21):e108–10.
25. Digre A, Lindskog C. The Human Protein Atlas - integrated omics for single cell mapping of the human proteome. Protein Sci. 2023;32(2): e4562.
26. Sun D, et al. TISCH: a comprehensive web resource enabling interactive single-cell transcriptome visualization of tumor microenvironment. Nucleic Acids Res. 2021;49(D1):D1420–30.
27. Molodtsov AK, et al. Resident memory CD8+ T cells in regional lymph nodes mediate immunity to metastatic melanoma. Immunity. 2021;54(9):2117-2132.e7.
28. Deng W, et al. Single-cell RNA-sequencing analyses identify heterogeneity of CD8+ T cell subpopulations and novel therapy targets in melanoma. Mol Ther Oncolytics. 2020;20:105–18.
29. Sabit I, et al. Binding of a sialic acid-recognizing lectin siglec-9 modulates adhesion dynamics of cancer cells via calpain-mediated protein Degradation. J Biol Chem. 2013;288(49):35417–27.
30. Wang J, et al. Siglec receptors modulate dendritic cell activation and antigen presentation to T cells in cancer. Front Cell Dev Biol. 2022;10:828916.
31. Beatson R, et al. The mucin MUC1 modulates the tumor immunological microenvironment through engagement of the lectin Siglec-9. Nat Immunol. 2016;17(11):1273–81.
32. Zhao F, et al. LINC01004-SPI1 axis-activated SIGLEC9 in tumor-associated macrophages induces radioresistance and the formation of immunosuppressive tumor microenvironment in esophageal squamous cell carcinoma. Cancer Immunol Immunother. 2023;72(6):1835–51.
33. Nirmal AJ, et al. The spatial landscape of progression and immunoediting in primary melanoma at single cell resolution. Cancer Discov. 2022;12(6):1518–41.

Publisher's Note